Journal of the Serbian Chemical Society
JSCS-info@shd.org.rs • www.shd.org.rs/JSCS
*J. Serb. Chem. Soc.* *85* (7) 953–965 (2020)
*JSCS–5351*
UDC 546.817.004.74+661.183.2:544.723:544.6.076.2–034
*Original scientific paper*

# Fixed bed adsorption treatment of effluent of battery recycling unit to remove Pb(II) using steam-activated granular carbon

SAURABH MESHRAM*, CHANDRAKANT THAKUR and ANUPAM B. SONI

*Department of Chemical Engineering, National Institute of Technology Raipur, 492010, Chhattisgarh, India*

(Received 3 November 2019, revised 4 February, accepted 2 March 2020)

*Abstract*: Battery recycling generates large amount of effluent which contains the toxic Pb(II) beyond the permissible limit. This effluent was treated for the removal of Pb(II) by fixed bed adsorption onto steam-activated granular carbon. Effect of flow rate, bed diameter and bed height on the performance of fixed bed column was investigated. The experimental data was presented in the form of breakthrough curve. Bed exhaustion time, breakthrough time and adsorbent capacity were determined. The obtained experimental data were evaluated with the four kinetic models: Thomas, Yoon–Nelson, Adams–Bohart and Clark model. The data were fitted well to the Thomas, Yoon–Nelson and Clark model with correlation coefficient $R^2 > 0.96$.

*Keywords*: lead removal; breakthrough curve; kinetic models; lead-acid battery; continuous adsorption.

## INTRODUCTION

Storage battery is the highest consumer of lead with more than 60% consumption of the total lead produced.[1] This demand of the lead for storage battery manufacturing is supplied by the secondary lead produced by recycling the battery.[2] Large amount of effluent generated during the recycling of battery which contains soluble Pb(II) in the range of 2–300 mg $L^{-1}$.[3] Pb(II) must be removed from the effluent before discharge, as it is considered as one of the most toxic heavy metal which upon exposure may cause serious health issues in human health like anemia, insomnia, dizziness, irritability and weakness of muscles. It can also damage the kidney, liver and reproductive system, basic cellular processes and brain functions upon exposure for longer duration.[4] Indian Standard Institution has recommended the maximum permissible limit of Pb(II) in drinking water is 0.05 mg $L^{-1}$ and that in surface water is 0.1 mg $L^{-1}$. According to

* Corresponding author. E-mail: smeshram.phd2016.chem@nitrr.ac.in
https://doi.org/10.2298/JSC191103015M

United States Environmental Protection Agency (USEPA) lead should be less than 0.015 mg $L^{-1}$ in drinking water.[5,6]

Effluent from battery recycling unit is treated conventionally by desulphurization using sodium carbonate, which gives the byproduct sodium sulphate and insoluble lead hydroxide and lead carbonate as sludge. Lead hydroxide formed during the treatment is not completely insoluble and can be found in discharge that needs to be removed. Some local battery recyclers are dumping the effluent without any treatment to save the cost of recycling.[3,7,8]

This effluent was treated by adsorption in the current study for the removal of lead because this method is economical, easy to operate and efficient to use. Various adsorbents were used previously to remove lead from aqueous solution, like bentonite, poly vinyl alcohol, carbon nanotube, chitosan, rice husk ash, bagasse fly ash and activated carbon.[9–16] Activated carbon has been chosen in this work because it is largely produced and widely used in water treatment.

For practical application of adsorption in water treatment continuous mode study or fixed bed study is need to be done. Fixed bed study is helpful in scaling up the column for water treatment application where various operational parameters are encountered.[17] The performance of the fixed-bed adsorption column system is generally described by the breakthrough curve and the shape of breakthrough curve is affected by the bed height, bed diameter, initial concentration and flow rate.[18] In the present study lead was removed from battery recycling unit effluent by the adsorption in fixed bed of steam-activated granular carbon (SGAC). Experiments were carried out to determine the effect of bed height, bed diameter and flow rate on percent removal of lead by SGAC. Experimental data were fitted to the Yoon–Nelson, Thomas, Adams–Bohart and Clark models to understand the adsorption phenomena.

## EXPERIMENTAL

### *Adsorbent and adsorbate*

SGAC of the size 1–2 mm was obtained from Indo German Carbons Limited, Kerala, India. Properties of SGAC were determined by FTIR (Bruker, Alpha Model), XRD (PANalytical multifunctional XRD analyzer) and SEM (ZEISS EVO). Various functional groups like O–H, C–H, C–O, C=C were found in the SGAC by FTIR analysis. SEM and XRD analysis revealed that the SGAC was having highly porous structure and amorphous in nature. Surface area found was 558 $m^2$ $g^{-1}$ by BET surface area analyzer (Smart sorb 93).

Effluent was collected from the local battery recycling unit located in Raipur, India. Collected effluent was found to contain Pb(II) and *COD* as 10.6 and 280 mg $L^{-1}$, respectively. Effluent was acidic in nature and neutralized with NaOH till the pH is 4.5 as this pH was found optimum by batch adsorption study.

### *Fixed bed column experiment*

A schematic representation of a fixed bed adsorption column using SGAC as adsorbent is shown in Fig. 1. Vertical acrylic columns of diameter 1.5, 3 and 4.5 cm were used in fixed-bed adsorption experiments. The effluent was pumped into the column from the top at the

flow rate of 4, 8 and 12 mL $min^{-1}$ using a peristaltic pump (Raveltech RH-P100S). The height of SGAC bed was fixed at 10, 20 and 30 cm. Experimental run has been performed to present the effect of highest and lowest value of one parameter while keeping the other parameter constant. The samples were collected from the bottom of the column at fixed time intervals. The remaining concentration of Pb(II) in effluent were determined using AAS (Atomic Absorption Spectrometer, Make-ECIL, India).

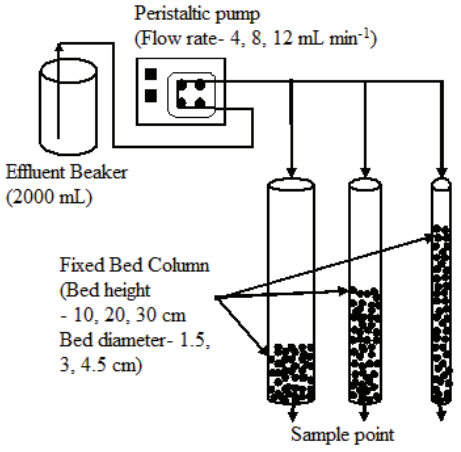


Fig.1. Schematic diagram of fixed bed experimental setup.

*Column data analysis*

Fixed-bed adsorption column performance was analyzed by the breakthrough curve. Breakthrough time and column exhaustion time was determined from the breakthrough curve.[19] Breakthrough time ($t_b$) was the point where treated effluent from the column was reached the predefined concentration (1 % of the influent concentration) and column exhaustion time ($t_c$) was taken as the time to reach the concentration of treated effluent 95 % of the initial concentration.[20]

Total volume of effluent from the column ($V$) after passing through adsorbent bed was calculated by multiplying the flow rate of influent ($Q$) and the total flow time $t$. Total mass of lead adsorbed ($q_{total}$) was obtained by calculating the area under the breakthrough curve given by Eq. (1):[21]

$$q_{total} = \frac{Q}{1000}\int_0^t (C_o - C_e)\,dt \quad (1)$$

where, $C_o$ is initial concentration of Pb(II) in the effluent and $C_e$ is the concentration of Pb(II) in the effluent at equilibrium.

Equilibrium uptake or maximum adsorbent capacity ($q_e$) of the column is defined as the ratio of total amount of lead adsorbed to the amount of adsorbent ($w$).[22] Total amount of lead passed from the column ($m_{total}$) at time $t$ and percentage removal of lead ($Y$) were determined by Eqs. (2) and (3):[23]

$$m_{total} = C_o Qt/1000 \quad (2)$$

$$Y = 100(q_{total}/m_{total}) \quad (3)$$

The empty bed contact time (*EBCT*) is the time of contact between the bed and adsorbate in the column defined as ratio of bed volume to flow rate. It is an important parameter for the

design of fixed bed column as it affects the breakthrough curve shape.[24] The performance of fixed bed adsorption column was further evaluated by the term adsorbent usage rate ($U_r$), which is defined as the ratio of weight of adsorbent in the bed ($w$) to the volume of effluent treated till breakthrough ($V_{Br}$).[25]

*Kinetic model for continuous mode of adsorption*

Concentration of the Pb(II) in adsorbent and effluent vary with the bed height and time during fixed bed adsorption. Kinetic models are used to understand the dynamic behaviour of fixed bed adsorption which helps in designing and optimization of process variables.[26] To evaluate the performance of column and adsorbent capacity following linear kinetic models were used.

*Thomas model*

Thomas model is based on the second-order reversible Langmuir kinetics of the adsorption process and assumes that there is no axial dispersion of sorbate in the fixed bed.[17] This model suggests that diffusion resistances are small enough to be negligible.[27] Eq. (4) presents linearized form of Thomas model:

$$\ln\left[\frac{C_o}{C_e}-1\right]=\frac{k_T q_T w}{Q}-k_T C_o t \tag{4}$$

where, $k_T$ is the Thomas model constant and $q_T$ is adsorption capacity.

*Yoon–Nelson model*

Yoon–Nelson model assumes that for each sorbate molecule to be adsorbed, the rate of decrease in the probability of adsorption is proportional to the probability of sorbate adsorption and breakthrough.[28] The linear form of Yoon–Nelson model expressed in Eq. (5):

$$\ln(\frac{C_e}{C_o-C_e})=k_{YN}t-\tau k_{YN} \tag{5}$$

where, $k_{YN}$ is rate velocity constant and $\tau$ is the time needed for 50 % adsorbate breakthrough.

*Adams–Bohart model*

Adams–Bohart model is based on the surface reaction theory and best suited for the initial part of the breakthrough curve. It is based on the assumption that the attainment of equilibrium is not instantaneous and the rate of adsorption is proportional to the adsorbent residual capacity and adsorbate concentration.[29] Adams–Bohart linear equation is given in Eq. (6):

$$\ln(\frac{C_e}{C_o})=k_{AB}C_o t-k_{AB}N_o\frac{L}{\mu} \tag{6}$$

where, $k_{AB}$ is Adams–Bohart rate constant, $N_o$ is equilibrium volumetric sorption capacity and $\mu$ is linear velocity of influent.

*Clark model*

This model is based on the combination of mass transfer concept and the assumption of Freundlich isotherm and assumes that no adsorption takes place at the start of the column and shape of the mass transfer zone is constant.[27] Linearized form of Clark model is given by Eq. (7):

$$\ln((\frac{C_o}{C_e})^{n-1}-1)=-rt+\ln A \tag{7}$$

where $n$ is the parameter of the Freundlich isotherm model, $r$ is the product of Clark model constant ($k_C$) and initial concentration of effluent ($C_o$) and $A$ is the constant given by Eq. (8):

$$A = \exp(\frac{k_C N_C L}{\mu}) \quad (8)$$

where $N_C$ is the removal capacity.

## RESULTS AND DISCUSSIONS

### *Effect of flow rate on breakthrough curve*

Table I shows the parameters for fixed bed adsorption of Pb(II) for different operating conditions. The breakthrough curves at the flow rate of 4 and 12 mL min$^{-1}$ are illustrated in Fig. 2 with the bed height of 20 cm and bed diameter of 1.5 and 4.5 cm.

TABLE I. Different parameters for fixed bed adsorption under different operating conditions

| Experiment conditions | | | $t_b$ | $t_e$ | $V_{Br}$ | $V$ | $EBCT$ | $U_r$ | $q_e$ | $Y$ |
|---|---|---|---|---|---|---|---|---|---|---|
| $Q$ /mL min$^{-1}$ | $L$ / cm | $D$ / cm | min | min | mL | mL | min | g L$^{-1}$ | mg g$^{-1}$ | % |
| **4** | 20 | 1.5 | 118 | 455 | 472 | 1820 | 8.83 | 0.04 | 0.08 | 6.91 |
| **12** | 20 | 1.5 | 32 | 148 | 384 | 1776 | 2.94 | 0.04 | 0.06 | 5.62 |
| **4** | 20 | 4.5 | 365 | 763 | 1460 | 3052 | 79.48 | 0.14 | 0.01 | 8.09 |
| **12** | 20 | 4.5 | 180 | 660 | 2160 | 7920 | 26.49 | 0.09 | 0.03 | 7.75 |
| 8 | **10** | 4.5 | 240 | 578 | 1920 | 4624 | 19.87 | 0.05 | 0.03 | 6.24 |
| 8 | **30** | 4.5 | 443 | 920 | 3544 | 7360 | 59.61 | 0.09 | 0.01 | 4.19 |
| 4 | **10** | 3 | 220 | 574 | 880 | 2296 | 17.66 | 0.05 | 0.07 | **11.94** |
| 4 | **30** | 3 | 360 | 820 | 1440 | 3280 | 52.99 | 0.09 | 0.02 | 7.50 |
| 8 | 10 | **1.5** | 82 | 250 | 656 | 2000 | 2.21 | 0.02 | **0.19** | 9.31 |
| 8 | 10 | **4.5** | 240 | 578 | 1920 | 4624 | 19.87 | 0.05 | 0.03 | 6.24 |
| 8 | 30 | **1.5** | 129 | 357 | 1032 | 2856 | 6.62 | 0.03 | 0.07 | 6.79 |
| 8 | 30 | **4.5** | 443 | 920 | 3544 | 7360 | 59.61 | 0.09 | 0.01 | 4.19 |

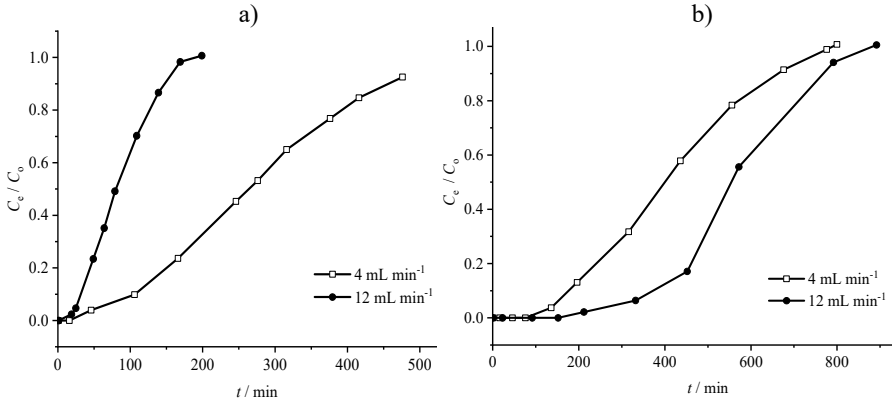


Fig. 2. Effect of flow rate on breakthrough curve for bed height 20 cm and bed diameter of: a) 1.5 and b) 4.5 cm.

It was observed from Fig. 2a that for higher flow rate the curve was steeper and the breakthrough time was lower. This might have resulted due to the fact that at high flow rates, SGAC saturates more quickly by being in contact with a large amount of Pb(II) ions.[21,30] It can be observed from Table I that the percentage removal of Pb(II) was lower at high flow rates. This might have been due to decreased residence time and higher Reynolds number, because of which Pb(II) did not get the sufficient time to make contact with the surface of the SGAC and diffusion coefficient reduced.[18] It was also observed from Fig. 2 that for the same flow rate of 12 mL $min^{-1}$, the breakthrough time increased from 35 to 180 min as the bed diameter increased from 1.5 to 4.5 cm. This might have resulted due to the availability of more adsorption sites to contact with the Pb(II) ions. Relatively small maximum adsorbent capacity of 0.19 mg $g^{-1}$ was found which might have due to the impurities presented in the real effluent of battery recycling unit.

*Effect of bed height on breakthrough curve*

Fig. 3 presents the effect of bed height 10 and 30 cm on the breakthrough curve for two different operating conditions flow rate 8 mL $min^{-1}$, bed diameter 4.5 cm and flow rate 4 mL $min^{-1}$, bed diameter 3 cm.

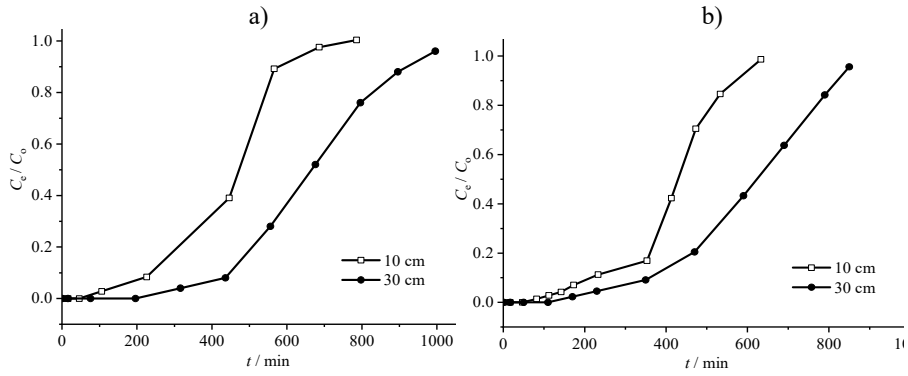


Fig. 3. Effect of bed height on breakthrough curve for: a) flow rate 8 mL $min^{-1}$ and bed diameter 4.5 cm and b) flow rate 4 mL $min^{-1}$ and bed diameter 3 cm.

It was observed that for the larger bed height the breakthrough time was increased and the saturation of adsorbent became slower because of the larger contact time caused by more adsorbent in bed and longer mass transfer zone.[31] It was observed from Table I that breakthrough time for flow rate 8 mL $min^{-1}$ and bed diameter 4.5 cm was less than that for flow rate 4 mL $min^{-1}$ and bed diameter 3 cm. This might have resulted due to less adsorption sites in the lower bed diameter.[30] It was also found from Table I that for the flow rate of 8 mL $min^{-1}$ and bed diameter of 4.5 cm, the adsorbent bed capacity was reduced from 0.03 to

0.01 mg $g^{-1}$, when the bed height increased from 10 to 30 cm. This might have resulted due to the increase in unused bed mass.

*Effect of bed diameter of breakthrough curve*

Effect of bed diameter on breakthrough curve is shown in Fig. 4. It was observed that the breakthrough time and the exhaustion time rose significantly with the increase in bed diameter. This might have resulted because of the fact that a larger number of SGAC existed along the cross sectional area of the column at a wider diameter column for binding the Pb(II) ions.[22] For the bed height of 10 cm and flow rate of 8 mL $min^{-1}$ the breakthrough time was decreased from 240 min to 82 min when the bed diameter increased from 4.5 cm to 1.5 cm. It indicated the decrease in mass transfer zone and the contact time for adsorption.[32]

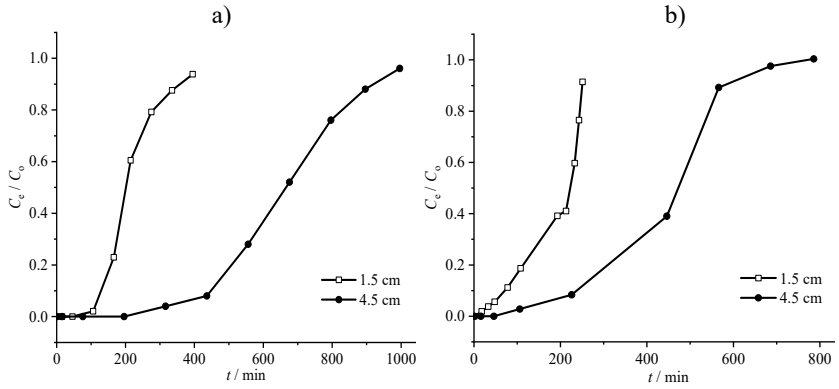


Fig. 4. Effect of bed diameter on breakthrough curve for flow rate 8 mL $min^{-1}$ and bed height of: a) 30 and b) 10 cm.

*Breakthrough curve modeling*

Data of the column studies were fitted to the linear form of Thomas, Yoon–Nelson, Adams–Bohart and Clark model. Kinetic parameters, correlation coefficient ($R^2$) and root mean square error (*RMSE*) are listed in Table II. Best fitting of the data in different models were in the order of Thomas > Yoon–Nelson > Clark > Adams–Bohart. Thomas model constant ($k_T$) and the adsorption capacity ($q_T$) were determined from the linear plot for different operating conditions (Fig. 5). It was observed that for the flow rate of 4 mL $min^{-1}$ the value of $k_T$ was 0.01 L $mg^{-1}$ $min^{-1}$, which was increased to 0.049 L $mg^{-1}$ $min^{-1}$ for the flow rate of 12 mL $min^{-1}$, while $q_T$ was decreased from 0.081 to 0.063 mg $g^{-1}$. This might have been due to the unavailability of the response sites.[18] The value of $q_T$ was in good agreement with the experimental value of adsorbent capacity ($q_e$), which confirmed the suitability of Thomas model.[22] The well fit of the experimental

data onto Thomas model indicated that the external and internal diffusion limitations were not present in the adsorption process.[19] The similar trends of results were obtained by Xu *et al*. for adsorption of nitrate by stratified wheat straw resin.[33]

TABLE II. Various parameters for Thomas, Yoon–Nelson, Adams–Bohart and Clark models derived from the fitting of experimental data

| Experiment conditions | | | Thomas model | | | | Yoon–Nelson model | | | |
|---|---|---|---|---|---|---|---|---|---|---|
| $Q$ mL min$^{-1}$ | $L$ cm | $D$ cm | $q_T$ mg g$^{-1}$ | $k_T$ L mg$^{-1}$ min$^{-1}$ | $R^2$ | *RMSE* | $k_{YN}$ min$^{-1}$ | $\tau$ min | $R^2$ | *RMSE* |
| 4 | 20 | 1.5 | 0.081 | 0.010 | 0.993 | 0.167 | 0.013 | 274.516 | 0.993 | 0.167 |
| 8 | 20 | 3 | 0.045 | 0.011 | 0.991 | 0.251 | 0.011 | 448.562 | 0.991 | 0.251 |
| 12 | 20 | 1.5 | 0.063 | 0.049 | 0.967 | 0.658 | 0.052 | 83.614 | 0.967 | 0.658 |
| 4 | 30 | 3 | 0.019 | 0.008 | 0.978 | 0.378 | 0.009 | 590.564 | 0.978 | 0.378 |
| 8 | 30 | 4.5 | 0.011 | 0.015 | 0.996 | 0.162 | 0.009 | 669.195 | 0.996 | 0.162 |
| 12 | 30 | 3 | 0.019 | 0.026 | 0.975 | 0.661 | 0.028 | 197.624 | 0.975 | 0.661 |
| | | | Adams–Bohart model | | | | Clark model | | | |
| | | | $N_o$ mg L$^{-1}$ | $k_{AB}$ L mg$^{-1}$ min$^{-1}$ | $R^2$ | *RMSE* | $k_C$ L mg$^{-1}$ min$^{-1}$ | $N_C$ mg L$^{-1}$ | $R^2$ | *RMSE* |
| 4 | 20 | 1.5 | 59.316 | 0.006 | 0.878 | 0.406 | 0.012 | 45.375 | 0.981 | 0.322 |
| 8 | 20 | 3 | 37.834 | 0.006 | 0.904 | 0.499 | 0.013 | 30.177 | 0.985 | 0.392 |
| 12 | 20 | 1.5 | 57.104 | 0.017 | 0.727 | 0.765 | 0.055 | 35.056 | 0.966 | 0.742 |
| 4 | 30 | 3 | 16.447 | 0.005 | 0.971 | 0.259 | 0.010 | 13.479 | 0.990 | 0.302 |
| 8 | 30 | 4.5 | 9.436 | 0.008 | 0.907 | 0.420 | 0.018 | 7.640 | 0.994 | 0.234 |
| 12 | 30 | 3 | 21.846 | 0.010 | 0.895 | 0.536 | 0.029 | 13.951 | 0.990 | 0.469 |

The rate velocity constant ($k_{YN}$) and the 50 % breakthrough time ($\tau$) for Yoon–Nelson model were determined from the linear plot (Fig. 6). The time ($\tau$), required to reach the 50 % breakthrough, was decreased from 274 to 83 min when the flow rate increased from 4 to 12 mL min$^{-1}$ due to faster saturation of the adsorbent bed.[34,35] The value of $\tau$ obtained from Yoon–Nelson model was

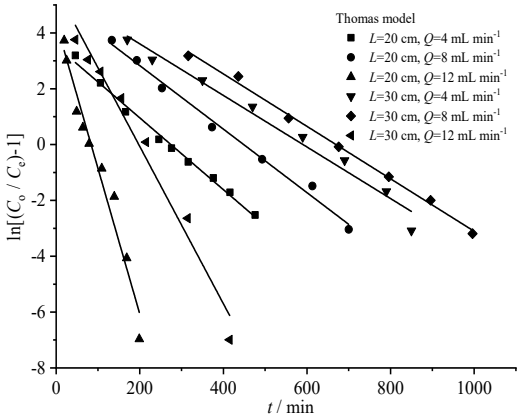


Fig. 5. Linear fit of experimental data for Thomas model.

almost similar to the value of experimental results. The correlation coefficient of more than 0.96 confirmed the suitability of Yoon–Nelson model for the adsorption of Pb(II) onto SGAC. Similar trends of results for Yoon–Nelson model were obtained by Aksu and Gonen, for continuous adsorption of phenol by the fixed bed of immobilized activated sludge.[36]

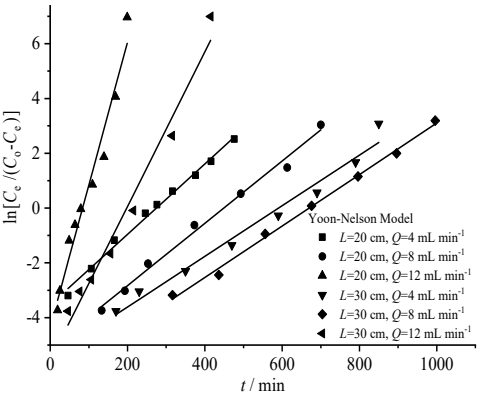


Fig. 6. Linear fit of experimental data for Yoon-Nelson model.

Adams–Bohart model provides simple approach for evaluation of fixed bed adsorption, but its applicability is limited to the narrow range of conditions.[33] The maximum adsorption capacity ($N_o$) and the kinetic constant ($k_{AB}$) for the Adams–Bohart model were determined from the linear plot (Fig. 7). It was observed that the Adams-Bohart model was fitted well ($R^2 > 0.9$) for the combination of low flow rate and high bed volume due increase in retention time. $N_o$ decreased with the increasing bed depth and flow rate, while the value of $k_{AB}$ rose with the increase in flow rate and decrease in bed depth. This result indicated that in the initial part of fixed bed adsorption kinetics of overall system was dominated by external mass transfer.[20] Similar results were obtained by Han *et al.* for the fixed bed adsorption of methylene blue by phoenix tree leaf powder.[37]

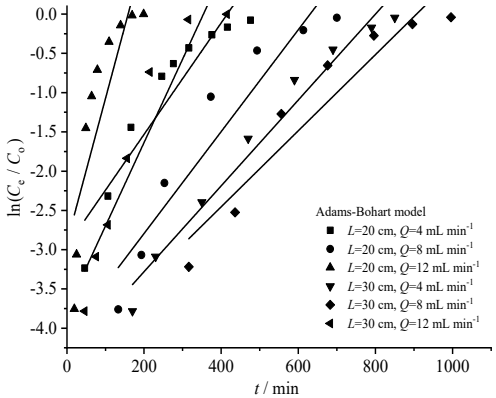


Fig.7. Linear fit of experimental data Adams–Bohart model.

Clark model constant ($k_C$) and removal capacity ($N_C$) was obtained from the linear plot (Fig. 8). Since the Freundlich isotherm kinetics was approximately valid for the batch adsorption of Pb(II) onto SGAC, Freundlich parameter ($1/n$ = = 0.41) was used to calculate the parameters of the Clark model.[37] It was observed from the Table II that an increase in flow rate from 4 to 12 mL min$^{-1}$, the value of $k_C$ was increased 0.012 to 0.055 L mg$^{-1}$ min$^{-1}$ and the value of $N_C$ decreased from 45.37 to 35.05 mg L$^{-1}$. Similar relationship between the $k_C$ and flow rate were obtained by Srivastava *et al.*[38] for the removal of phenol by bagasse fly ash. High correlation coefficient of more than 0.93 showed the applicability of Clark model for the fixed bed adsorption of Pb(II) onto SGAC.

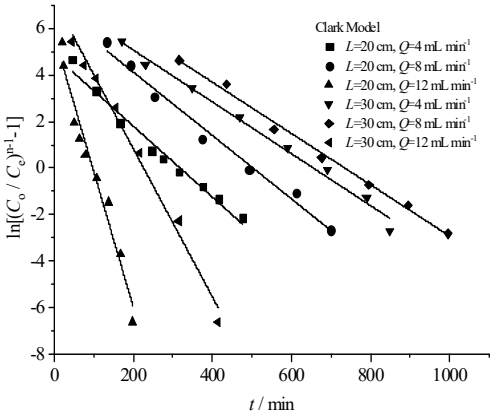


Fig. 8. Linear fit of experimental data for Clark model.

Out of the four models, only Thomas, Yoon–Nelson and Clark models were fitted well to the experimental data with high $R^2$ value and low *RMSE*, while Adams–Bohart model was not showing the satisfactory prediction of the adsorption performance. Similar results for the models were obtained by Dhanasekaran *et al.* for the fixed bed adsorption study of fluoride by *Artocarpus hirsutus* based adsorbent.[27]

## CONCLUSIONS

The performance of fixed bed column using SGAC has been investigated for the treatment of effluent of battery recycling unit in terms of flow rate, bed height and bed diameter. Breakthrough time, uptake capacity and percentage of removal of lead were used as parameters for evaluating the adsorption performances. For the higher flow rate, the lower breakthrough time and percentage of removal were observed, while the uptake capacity depends on the *D*/*L* ratio. The increase in both bed height and bed diameter results in increase of breakthrough time and decrease in uptake capacity and the percentage of lead removal. The maximum adsorbent capacity found was 0.19 mg g$^{-1}$ for the flow rate of 8 mL min$^{-1}$, the column height of 10 cm and the column diameter of 1.5 cm. The adsorption kin-

etic models were applied to the experimentally obtained data in order to understand the adsorption mechanism. The Thomas model fitted well to the experimental data, which indicated that the internal and external diffusions were not the limiting phenomena for adsorption. The Yoon–Nelson model with the correlation coefficient $R^2 > 0.96$ estimated the time for 50 % breakthrough which is almost identical to the experimental results. The Clark model also fitted well to the experimental data, which confirmed that the batch adsorption of Pb(II) onto SGAC follows the Freundlich isotherm. Furthermore, further study about desorption and regeneration under different conditions should be performed and taken into consideration. This work suggests a possible alternative treatment method for the removal of Pb(II) from effluent from the battery recycling unit.

*Acknowledgements.* The authors want to acknowledge the support and facilities provided by National Institute of Technology Raipur, India. The author also wants to acknowledge the Guru Ghasidas University Bilaspur, India, for granting the study leave to do Ph.D.

ИЗВОД

## УКЛАЊАЊЕ Pb(II) ИЗ ИЗЛАЗНОГ ТОКА ЈЕ ДИНИЦЕ ЗА РЕЦИКЛАЖУ БАТЕРИЈА АДСОРПЦИЈОМ НА ГРАНУЛИСАНОМ АКТИВНОМ УГЉУ АКТИВИРАНОГ ПАРОМ У ПАКОВАНОМ СЛОЈУ

SAURABH MESHRAM, CHANDRAKANT THAKUR и ANUPAM B SONI

*Department of Chemical Engineering, National Institute of Technology Raipur, 492010, Chhattisgarh, India*

Рециклажа батерија производи велике количине отпадног тока које садрже токсични Pb(II) изнад прописаних граница. Овај отпадни ток је третирана ради уклањања Pb(II) адсорпцијом на гранулисаном активном угљу активираног паром у пакованом слоју. Испитиван је утицај запреминског протока, пречника и висине слоја на перформансе адсорпционе колоне. Експериментални подаци су приказани у облику кривих пробоја. Одређни су време исцрпљења адсорпционог слоја, време пробоја и адсорпциони капацитет. За евалуацију добијених експерименталних података коришћена су 4 кинетичка модела: Thomas, Yoon–Nelson, Adams–Bohart и Clark модел. Thomas, Yoon––Nelson и Clark модел су показали добро слагање са експерименталним подацима, са корелационим коефицијентом $R^2 > 0{,}96$.

(Примљено 3. новембра 2019, ревидирано 4. фебруара, прихваћено 2. марта 2020)

## REFERENCES

1. Y. Gong, J. E. Dutrizac, T. T. Chen, *Hydrometallurgy* **28** (1992) 399 (https://doi.org/10.1016/0304-386X(92)90044-Z)
2. J. Zhang, C. Chen, X. Zhang, S. Liu, *Procedia Environ. Sci.* **31** (2016) 873 (https://doi.org/10.1016/j.proenv.2016.02.103)
3. W. Zhang, J. Yang, X. Wu, Y. Hu, W. Yu, J. Wang, J. Dong, M. Li, S. Liang, J. Hu, R.V. Kumar, *Renew. Sustain. Energy Rev.* **61**(2016)108 (https://doi.org/10.1016/j.rser.2016.03.046)
4. R. Naseem, S. S. Tahir, *Wat. Res.* **35** (2001) 3982
5. M. Momcilovic, M. Purenovic, A. Bojic, A. Zarubica, M. Ranđelović, *Desalination* **276** (2011) 53 (https://doi.org/10.1016/j.desal.2011.03.013)

6. H. M. Albishri, H. M. Marwani, E. M. Soliman, *Arab. J. Chem.* **10** (2017) S1955 (http://dx.doi.org/10.1016/j.arabjc.2013.07.023)
7. G. Macchi, M. Pagano, M. Santori, G. Tiravanti, *Wat. Res*. **27** (1993) 1511 (https://doi.org/10.1016/0043-1354(93)90095-Y)
8. T. Bahadir, G. Bakan, L. Altas, H. Buyukgungor, *Enz. Microb. Technol.* **41** (2007) 98 (https://doi.org/10.1016/j.enzmictec.2006.12.007)
9. N. H. Yarkandi, Int. J. Curr. Microbiol. *App. Sci.* **3** (2014) 207
10. J. Haiyan, Z. Qiuxiang, Z. Ying, *Desalin. Water Treat.* (2015) 1 (https://doi.org/10.1080/19443994.2015.1006258)
11. V. K. Gupta, S. Agarwal, T. A. Saleh, *J. Hazard. Mater.* **185** (2011) 17 (https://doi.org/10.1016/j.jhazmat.2010.08.053)
12. A. R. Fajardo, L. C. Lopes, A. F. Rubira, E. C. Muniz, *Chem. Eng. J.* **183** (2012) 253 (http://dx.doi.org/10.1016/j.cej.2011.12.071)
13. V. C. Srivastava, I. D. Mall, I. M. Mishra, *J. Hazard. Mater.* **134** (2006) 257 (https://doi.org/10.1016/j.jhazmat.2005.11.052)
14. V. K. Gupta, I. Ali, *J. Colloid Interface Sci.* 271 (2004) 321 (https://doi.org/10.1016/j.jcis.2003.11.007)
15. R. Ayyappan, A. C. Sophia, K. Swaminathan, S. Sandhya, *Proc. Biochem.* **40** (2005) 1293 (https://doi.org/10.1016/j.procbio.2004.05.007)
16. R. R. Bansode, J. N. Losso, W. E. Marshall, R. M. Rao, R. J. Portier, *Bioresour. Technol.* **89** (2003) 115 (https://doi.org/10.1016/S0960-8524(03)00064-6)
17. M. Basu, A. K. Guha, L. Ray, *Bioresour. Technol.* **283** (2019) 86 (https://doi.org/10.1016/j.biortech.2019.02.133)
18. J. Qu, T. Song, J. Liang, X. Bai, Y. Li, Y. Wei, S. Huang, L. Dong, *Ecotoxicol. Environ. Saf.* **169** (2019) 722 (https://doi.org/10.1016/j.ecoenv.2018.11.085)
19. S. Chen, Q. Yue, B. Gao, Q. Li, X. Xu, K. Fu, *Bioresour. Technol.* **113** (2012) 114 (https://doi.org/10.1016/j.biortech.2011.11.110)
20. T. Zang, Z. Cheng, L. Lu, Y. Jin, X. Xu, W. Ding, J. Qu, *Ecol. Eng.* **99** (2017) 358 (https://doi.org/10.1016/j.ecoleng.2016.11.070)
21. G. Nazari, H. Abolghasemi, M. Esmaieli, E. S. Pouya, *Appl. Surf. Sci.* **375** (2016) 144 (https://doi.org/10.1016/j.apsusc.2016.03.096)
22. A. A. Ahmad, B. H. Hameed, *J. Hazard. Mater.* **175** (2010) 298 (https://doi.org/10.1016/j.jhazmat.2009.10.003)
23. R. Sharma, B. Singh, *Bioresour. Technol.* **146** (2013) 519 (https://doi.org/10.1016/j.biortech.2013.07.146)
24. A. Tor, N. Danaoglu, G. Arslan, Y. Cengeloglu, *J. Hazard. Mater.* **164** (2009) 271 (https://doi.org/10.1016/j.jhazmat.2008.08.011)
25. E. Malkoc, Y. Nuhoglu, M. Dundar, *J. Hazard. Mater.* **138** (2006) 142 (https://doi.org/10.1016/j.jhazmat.2006.05.051)
26. A. Abdolali, H. H. Ngo, W. Guo, J. L. Zhou, J. Zhang, S. Liang, S. W. Chang, D. D. Nguyen, Y. Liu, *Bioresour. Technol.* **229** (2017) 78 (https://doi.org/10.1016/j.biortech.2017.01.016)
27. P. Dhanasekaran, P. M. S. Sai, K. I. Gnanasekar, *J. Fluor. Chem.* **195** (2017) 37 (https://doi.org/10.1016/j.jfluchem.2017.01.003)
28. F. Fadzil, S. Ibrahim, M. A. K. M. Hanafiah, *Process Saf. Environ. Prot.* **100** (2016) 1 (https://doi.org/10.1016/j.psep.2015.12.001)
29. P. Liao, Z. Zhan, J. Dai, X. Wu, W. Zhang, K. Wang, S. Yuan, *Chem. Eng. J.* **228** (2013) 496 (https://doi.org/10.1016/j.cej.2013.04.118)

30. T. A. H. Nguyen, H. H. Ngo, W. S. Guo, T. Q. Pham, F. M. Li, T. V Nguyen, X. T. Bui, *Sci. Total Environ.* **523** (2015) 40 (https://doi.org/10.1016/j.scitotenv.2015.03.126)
31. M. T. Bai, P. Venkateswarlu, *Mater. Today Proc.* **5** (2018) 18024 (https://doi.org/10.1016/j.matpr.2018.06.136)
32. S. Chatterjee, S. Mondal, S. De, *J. Clean. Prod.* **177** (2018) 760 (https://doi.org/10.1016/j.jclepro.2017.12.249)
33. X. Xu, B. Gao, X. Tan, X. Zhang, Q. Yue, Y. Wang, Q. Li, *Chem. Eng. J.* **226** (2013) 1 (https://doi.org/10.1016/j.cej.2013.04.033)
34. S. T. Song, Y. F. Hau, N. Saman, K. Johari, S. C. Cheu, H. Kong, H. Mat, *J. Environ. Chem.Eng.* **4** (2016) 1685 (https://doi.org/10.1016/j.jece.2016.02.033)
35. M. Auta, B. H. Hameed, *Chem. Eng. J.* **237** (2014) 352 (https://doi.org/10.1016/j.cej.2013.09.066)
36. Z. Aksu, F. Gönen, *Proc. Biochem.* **39** (2004) 599 (https://doi.org/10.1016/S0032-9592(03)00132-8)
37. R. Han, Y. Wang, X. Zhao, Y. Wang, F. Xie, J. Cheng, M. Tang, *DES* **245** (2009) 284 (https://doi.org/10.1016/j.desal.2008.07.013)
38. V. C. Srivastava, B. Prasad, I. M. Mishra, I. D. Mall, M. M. Swamy, *Ind. Eng. Chem. Res.* **47** (2008) 1603 (https://doi.org/10.1021/ie0708475).